

Deterministic photon entangler using a charged quantum dot inside a microcavity

C. Y. Hu,^{1,*} W. J. Munro,^{2,3} and J. G. Rarity¹

¹*Department of Electrical and Electronic Engineering, University of Bristol, University Walk, Bristol BS8 1TR, United Kingdom*

²*Hewlett-Packard Laboratories, Filton Road, Stoke Gifford, Bristol BS34 8QZ, United Kingdom*

³*National Institute of Informatics, 2-1-2 Hitotsubashi, Chiyoda-ku, Tokyo 101-8430, Japan*

(Received 15 August 2008; published 16 September 2008)

We present a deterministic and scalable scheme to generate photon polarization entanglement via a single electron spin confined in a charged quantum dot inside a microcavity. This scheme is based on giant circular birefringence and giant Faraday rotation induced by a single electron spin. Two independent photons are sequentially sent to the cavity and get entangled after measuring the spin state. We show that this scheme can be extended to generate multiphoton polarization entanglement including Greenberger-Horne-Zeilinger states and cluster states in a deterministic way.

DOI: [10.1103/PhysRevB.78.125318](https://doi.org/10.1103/PhysRevB.78.125318)

PACS number(s): 78.67.Hc, 03.67.Mn, 42.50.Pq, 78.20.Ek

I. INTRODUCTION

Entanglement lies at the heart of quantum mechanics and is a fundamental resource in quantum information science especially for quantum communications, quantum computation, quantum metrology, and quantum networks.^{1,2} Entanglement has been demonstrated in various quantum systems, among which photons are well investigated as an ideal candidate to transmit quantum information and even for quantum information processing.³ There exist three main ways to generate polarization entangled photon pairs. One way is via spontaneous parametric processes in nonlinear crystals or fibers where nondeterministic photon pairs are created.^{4,5} The second way is via radiative quantum cascades in a single atom⁶ or biexciton in a semiconductor quantum dot (QD),^{7,8} by which deterministic photon pairs are generated. A third way is via single-photon mixing at a nonpolarizing beam splitter followed by coincidence measurement.^{9,10} These methods require quantum interference through photon or path indistinguishability. Starting from entangled photon pairs, multiphoton entanglement can be built but this involves the use of nondeterministic and low-efficiency interference-based gates. This approach is ultimately not scalable and to our knowledge the current record is six-photon entanglement.¹¹

In this paper, we show that we can make entangled photon pairs and multiphotons in a deterministic and thus scalable way. We exploit our previous work on giant optical Faraday rotation induced by a single electron spin confined on a charged quantum dot with excitonic transition strongly coupled to a microcavity.¹² Independent photons are sent sequentially to probe a single microcavity containing a single electron spin in a superposition state. After measuring the spin state, we get entangled photon-pair states or in general N -photon Greenberger-Horne-Zeilinger (GHZ) states. This scheme is deterministic and thus scalable in principle to high N . It relies on path interference but does not necessarily need indistinguishable photons. Following similar procedures, a deterministic scheme for a photon-spin quantum interface could be implemented. These deterministic multiphoton entangler and photon-spin quantum interface are two essential components for solid-state quantum networks with single photons and single QD spins.

II. PHOTON-SPIN ENTANGLING OPERATOR

The optical properties of singly charged QDs are dominated by the optical transitions of the negatively charged exciton (X^-) that consists of two electrons bound to one hole.¹³ Due to the Pauli's exclusion principle, X^- shows spin-dependent optical transitions:¹⁴ the left-handed circularly polarized photon (marked by $|L\rangle$ or L photon) only couples to the electron in the spin state $|\uparrow\rangle$ to X^- in the spin state $|\uparrow\downarrow\uparrow\rangle$ with the two antiparallel electron spins; the right-handed circularly polarized photon (marked by $|R\rangle$ or R photon) only couples to the electron in the spin state $|\downarrow\rangle$ to X^- in the spin state $|\uparrow\downarrow\downarrow\rangle$. Here $|\uparrow\rangle$ and $|\downarrow\rangle$ represent electron-spin states $|\pm\frac{1}{2}\rangle$, and $|\uparrow\uparrow\rangle$ and $|\downarrow\downarrow\rangle$ represent heavy-hole spin states $|\pm\frac{3}{2}\rangle$. The spin-quantization axis is along the normal direction of cavity.

However, the above spin selection rule only holds for an ideal QD that is symmetric in both the QD shape and the strain field distribution so that there is no spin-level mixing or splitting. A realistic QD that is generally asymmetric can be made symmetric by applying an electric field,¹⁵ thermal annealing,¹⁶ or tuning the QD size.¹⁷ This spin selection rule for X^- transitions has been demonstrated in quantum wells¹⁴ and QDs.^{13,18,19} Hole mixing in a realistic QD can also affect the above selection rule. However, the hole mixing [e.g., for self-assembled In(Ga)As QDs] is in the order of a few percent and can be reduced by engineering the shape and size of QDs or by using different types of QDs.^{20,21}

We consider a singly charged QD, e.g., a self-assembled In(Ga)As QD or a GaAs interface QD inside an optical resonant cavity. Figure 1 shows a micropillar cavity where the two GaAs/Al(Ga)As distributed Bragg reflectors (DBR) and the transverse index guiding provide the three-dimensional confinement of light. Only the single-sided cavity is considered here: The bottom DBR is 100% reflective while the top DBR is partially reflective in order to couple the light into and out of the cavity. The QD is located at the antinodes of the cavity field to achieve optimized light-matter coupling. By solving the Heisenberg equations of motions for the cavity-field operator (\hat{a} and X^-) and dipole operator (σ_-) in the weak excitation approximation, we can obtain the reflection coefficient¹²

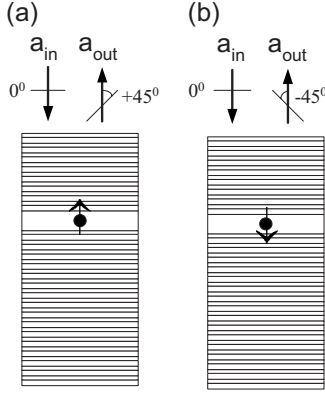


FIG. 1. Schematic of a quantum nondemolition measurement of a single electron spin based on giant optical Faraday rotation. To realize an ideal quantum measurement, the Faraday rotation angle is tuned to be $\pm 45^\circ$ (corresponding to a phase shift $\Delta\varphi = \pm \pi/2$) by setting $\omega - \omega_c \approx \pm \kappa/2$.

$$r(\omega) \equiv |r(\omega)|e^{i\varphi(\omega)} = 1 - \frac{\kappa \left[i(\omega_{X^-} - \omega) + \frac{\gamma}{2} \right]}{\left[i(\omega_{X^-} - \omega) + \frac{\gamma}{2} \right] \left[i(\omega_c - \omega) + \frac{\kappa}{2} + \frac{\kappa_s}{2} \right] + g^2}, \quad (1)$$

where $|r(\omega)|$ is the reflectance and $\varphi(\omega)$ is the phase shift. ω , ω_c , and ω_{X^-} are the frequencies of external field (probe beam), cavity mode, and X^- transition, respectively. g is the coupling strength between X^- and the cavity mode. $\gamma/2$ is the X^- dipole decay rate, and $\kappa/2$ and $\kappa_s/2$ are the cavity-field decay rates into the input/output modes and the leaky modes, respectively. For simplicity we use the following shorthand notation. If the QD couples to the cavity, we call it a hot cavity; if the QD does not couple to the cavity, we call it a cold cavity.

By taking $g=0$, we get the reflection coefficient for a cold cavity with QD uncoupled to the cavity,

$$r_0(\omega) = \frac{i(\omega_c - \omega) - \frac{\kappa}{2} + \frac{\kappa_s}{2}}{i(\omega_c - \omega) + \frac{\kappa}{2} + \frac{\kappa_s}{2}}. \quad (2)$$

The side leakage (and background absorption) can be made rather small by optimizing the etching process (or improving the sample growth) as reported recently.²² Therefore, we neglect the side leakage first in the following discussions but come back to it later.

For the cold cavity, we get near-unity reflectance $|r_0(\omega)| \approx 1$ and $\varphi_0(\omega) = \pm \pi + 2 \arctan 2(\omega - \omega_c)/\kappa$, where “+” stands for the case of $\omega \leq \omega_c$ and “-” stands for $\omega \geq \omega_c$ with ω_c as the cavity-mode frequency. $\varphi_0(\omega)$ can be tuned between $-\pi$ and π by varying the frequency detuning ($\omega - \omega_c$).

For the hot cavity where X^- strongly couples to the cavity, i.e., $g > (\kappa, \gamma)$, we get $|r_h(\omega)| \approx 1$ and $\varphi_h(\omega) \approx 0$ within a fre-

quency window $|\omega - \omega_c| \ll g$. The near-unity reflectance is due to the formation of the mixed X^- -cavity modes. The strongly coupled QD-cavity system has been demonstrated recently in various microcavities and nanocavities.²³⁻²⁵ For micropillars with diameter around $1.5 \mu\text{m}$, the coupling strength $g = 80 \mu\text{eV}$ and the quality factor of more than 4×10^4 (corresponding to $\kappa = 33 \mu\text{eV}$) have been reported^{22,23} indicating $g/\kappa = 2.4$ is already achievable for the In(Ga)As QD-cavity system. γ is about several μeV .

If the single excess electron lies in the spin state $|\uparrow\rangle$, the L photon feels a hot cavity and gets a phase shift of $\varphi_h(\omega)$ after reflection, whereas the R photon feels the cold cavity and gets a phase shift of $\varphi_0(\omega)$. Conversely, if the electron lies in the spin state $|\downarrow\rangle$, the R photon feels a hot cavity and gets a phase shift of $\varphi_h(\omega)$ after reflection, whereas the L photon feels the cold cavity and gets a phase shift of $\varphi_0(\omega)$. We call this phenomenon giant circular birefringence (GCB), which results in giant Faraday rotation (GFR) of linearly polarized light. Both GCB and GFR are induced by a single electron spin due to cavity QED and the optical spin selection rule of X^- transitions. GFR provides a quantum nondemolition measurement of a single electron spin (see Fig. 1), whereas GCB could be used to make a photon-spin entangling gate. The reflection operator can be written as

$$\hat{r}(\omega) = |r_0(\omega)|e^{i\varphi_0}(|R\rangle\langle R| \otimes |\uparrow\rangle\langle\uparrow| + |L\rangle\langle L| \otimes |\downarrow\rangle\langle\downarrow|) + |r_h(\omega)|e^{i\varphi_h}(|L\rangle\langle L| \otimes |\uparrow\rangle\langle\uparrow| + |R\rangle\langle R| \otimes |\downarrow\rangle\langle\downarrow|). \quad (3)$$

For $|r_0(\omega)| \approx 1$ and $|r_h(\omega)| \approx 1$ as discussed above [or for balanced reflectance $|r_h(\omega)| = |r_0(\omega)|$], the reflection operator can be simplified as $\hat{r}(\omega) = |r_0(\omega)|e^{i\varphi_0}\hat{U}(\Delta\varphi)$, where $\hat{U}(\Delta\varphi)$ is the phase-shift operator defined as

$$\hat{U}(\Delta\varphi) = e^{i\Delta\varphi(|L\rangle\langle L| \otimes |\uparrow\rangle\langle\uparrow| + |R\rangle\langle R| \otimes |\downarrow\rangle\langle\downarrow|)}, \quad (4)$$

where $\Delta\varphi = \varphi_h - \varphi_0$.

Unless otherwise specified, we set $\Delta\varphi = \pi/2$ by adjusting $\omega - \omega_c \approx \kappa/2$ in this paper. Before showing that this photon-spin entangling gate could be used to generate multiphoton entanglement, we discuss some conditions to apply the phase operator: (1) Numerical calculations show that $\Delta\varphi = \pi/2$ is achievable when $g > 1.5\kappa$ if $\kappa \gg \kappa_s$. This condition can be experimentally achieved as discussed above. (2) The photon pulse bandwidth $\Delta\omega$ should be much less than the cavity-mode broadening κ . This allows the frequency detuning ($\omega - \omega_c$) to be precisely set and consequently the phase shift $\Delta\varphi$ to be well defined. The photon pulse shape then remains unchanged after reflection. This demands that $|\partial\Delta\varphi/\partial\omega|_{\omega_0}\Delta\omega \ll \pi/2$, which is satisfied when $\Delta\omega \ll \kappa/2$, where ω_0 is the central frequency of the photon pulse. This kind of single-photon pulses can come from QD single-photon sources²⁶⁻²⁸ (the photon indistinguishability is not necessarily required as discussed below) or from nanosecond laser pulses. (3) Finally we require good mode matching between the traveling photons and the cavity as this will minimize the photon loss. However, we think this loss has the same effect on both the cold cavity and the hot cavity, so

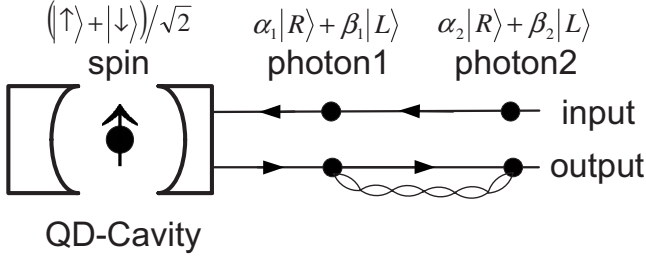


FIG. 2. A proposed scheme to generate polarization entanglement between independent photons via a single electron spin confined in a QD.

$|r_0(\omega)| = |r_h(\omega)|$ still holds and the phase operator $\hat{U}(\Delta\varphi)$ still works but with reduced gate success probability due to the photon loss.

III. PHOTON ENTANGLER

In Fig. 2, photon 1 in the state $|\psi^{\text{ph}}\rangle_1 = \alpha_1|R\rangle_1 + \beta_1|L\rangle_1$ and photon 2 in the state $|\psi^{\text{ph}}\rangle_2 = \alpha_2|R\rangle_2 + \beta_2|L\rangle_2$ are input into the cavity in sequence.²⁹ Both photons have the same frequency. The electron spin in the QD is prepared in a superposition state $|\psi^s\rangle = \frac{1}{\sqrt{2}}(|\uparrow\rangle + |\downarrow\rangle)$ and the phase-shift operator for the QD-cavity system is described by Eq. (4) with $\Delta\varphi = \pi/2$. After reflection, the photon states become entangled with the spin state, and the corresponding state transformation is

$$\begin{aligned} (\alpha_1|R\rangle_1 + \beta_1|L\rangle_1) \otimes (\alpha_2|R\rangle_2 + \beta_2|L\rangle_2) \otimes (|\uparrow\rangle + |\downarrow\rangle) \xrightarrow{\hat{U}(\pi/2)} & (|\uparrow\rangle \\ & - |\downarrow\rangle)[\alpha_1\alpha_2|R\rangle_1|R\rangle_2 - \beta_1\beta_2|L\rangle_1|L\rangle_2] + i(|\uparrow\rangle + |\downarrow\rangle) \\ & \times [\alpha_1\beta_2|R\rangle_1|L\rangle_2 + \alpha_2\beta_1|L\rangle_1|R\rangle_2]. \end{aligned} \quad (5)$$

By applying a Hadamard gate on the electron spin (e.g., using a $\pi/2$ microwave pulse), the two spin superposition states can be rotated to the states $|\uparrow\rangle$ and $|\downarrow\rangle$. Now the electron-spin states can be measured by the GFR-based quantum nondemolition method shown in Fig. 1. Photon 3 in the state $(|R\rangle_3 + |L\rangle_3)/\sqrt{2}$ is input into the cavity (photon 3 has the same frequency as photons 1 and 2) (Ref. 30); after reflection, the total state for the three photons and one spin becomes

$$\begin{aligned} (|R\rangle_3 + i|L\rangle_3)|\uparrow\rangle[\alpha_1\alpha_2|R\rangle_1|R\rangle_2 - \beta_1\beta_2|L\rangle_1|L\rangle_2] \\ - (|R\rangle_3 - i|L\rangle_3)|\downarrow\rangle[\alpha_1\beta_2|R\rangle_1|L\rangle_2 + \alpha_2\beta_1|L\rangle_1|R\rangle_2]. \end{aligned} \quad (6)$$

The output state of photon 3 can be measured in orthogonal linear polarizations. If the photon 3 is detected in the $|R\rangle_3 + i|L\rangle_3$ state (45° linear), so the electron spin is definitely in the state $|\uparrow\rangle$, and we project Eq. (6) onto an entangled photon state.

$$|\Phi_{12}^{\text{ph}}\rangle = \alpha_1\alpha_2|R\rangle_1|R\rangle_2 - \beta_1\beta_2|L\rangle_1|L\rangle_2. \quad (7)$$

On detecting the photon 3 in the $|R\rangle_3 - i|L\rangle_3$ state (-45° linear), so the spin is definitely in the state $|\downarrow\rangle$, and we project Eq. (6) onto another entangled photon state

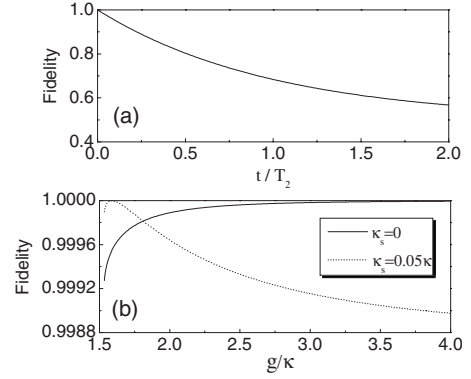


FIG. 3. (a) Entanglement fidelity vs the time interval between two photons. T_2 is the QD spin-coherence time. (b) Entanglement fidelity vs the coupling strength without side leakage (solid) and with side leakage included (dotted). We take $g/\kappa = 2.4$ and $\gamma/\kappa = 0.1$, which are experimentally achievable (see text). The curves are cut off for $g < 1.5\kappa$ as $\varphi_h(\omega) - \varphi_0(\omega) = \pm\pi/2$ cannot be achieved in this regime.

$$|\Psi_{12}^{\text{ph}}\rangle = \alpha_1\beta_2|R\rangle_1|L\rangle_2 + \alpha_2\beta_1|L\rangle_1|R\rangle_2. \quad (8)$$

On setting the coefficients $\alpha_{1,2}$ and $\beta_{1,2}$ to $1/\sqrt{2}$, we get maximally entangled photon states.

Although photons 1 and 2 never meet before, each of them gets entangled with the electron spin after sequentially interacting with the spin. The spin measurement then projects the two photons into entangled states. This entanglement-by-projection scheme, well known in mesoscopic systems,³¹ does not require photon indistinguishability or photon interference as demanded by other schemes using photon mixing on a beam splitter.^{9,10} For instance, we could even generate polarization entanglement between photons with different pulse length or different arrival time. The arrival-time difference between photons could be any time shorter than the electron-spin coherence time in QDs, which is ideal for quantum relay type applications. Recent experiments have shown that GaAs or In(Ga)As single QDs have long electron-spin coherence time ($T_2 \sim \mu\text{s}$),³² which is limited by the spin-relaxation time ($T_1 \sim \text{ms}$).³³ Due to the spin decoherence at time t ($t \ll T_1$), the density matrix of the electron spin in the initial state $|\psi^s\rangle = \frac{1}{\sqrt{2}}(|\uparrow\rangle + |\downarrow\rangle)$ becomes

$$\rho(t) = \begin{pmatrix} 1/2 & e^{-t/T_2}/2 \\ e^{-t/T_2}/2 & 1/2 \end{pmatrix}, \quad (9)$$

which represents a spin-mixed state. As a result, the entanglement fidelity with respect to Eq. (7) or (8) becomes

$$F = (1 + e^{-t/T_2})/2, \quad (10)$$

which decreases with t as shown in Fig. 3(a). Therefore high-fidelity photon entanglement can only be achieved when the time interval between two photons is much shorter than the spin-coherence time ($T_2 \sim \mu\text{s}$) in the QD.

The QD spin eigenstate can be prepared, for example, by optical pumping and/or optical cooling.^{18,34} From the spin basis state, there are two ways to get the spin superposition state: either via spin-flip Raman transitions¹⁸ or by perform-

ing single-spin rotations using nanosecond electron spin resonance (ESR) microwave pulses.³² Recently, ultrafast optical coherent control of electron spins has been reported in semiconductor quantum wells on femtosecond time scales and in semiconductor QDs on the picosecond time scales,³⁵ which are much shorter than the QD spin-coherence time ($T_2 \sim \mu\text{s}$). This allows ultrafast $\pi/2$ spin rotation required in our scheme.

If we neglect any other photon loss, such as mode mismatching, diffraction, and inefficient detection, our scheme is deterministic and scalable. For example, we could create GHZ states: first entangle photons 1 and 2 by interacting with the electron spin in its initial state $|\psi^s\rangle = \frac{1}{\sqrt{2}}(|\uparrow\rangle + |\downarrow\rangle)$ and then measuring the spin state. After setting the electron spin back to its initial state, we could entangle photons 2 and 3 in the same way. Now photons 1, 2, and 3 are in one of tripartite GHZ states $|\Psi_{123}\rangle = (|D\rangle_1|D\rangle_2|D\rangle_3 \pm |\bar{D}\rangle_1|\bar{D}\rangle_2|\bar{D}\rangle_3)/\sqrt{3}$ depending on spin-measurement results (all coefficients α 's and β 's are set to $1/\sqrt{2}$). Following this way, arbitrary N -photon GHZ states could be produced deterministically. Compared with other GHZ schemes, our scheme is not limited by the brightness and photon indistinguishability of entangled photon-pair sources.¹¹ If we sequentially entangle pairs of photons by repeating the above single-spin measurement scheme, which leads to Eqs. (7) and (8), we can also generate cluster states.³⁶

If the cavity side leakage is neglected, then our entanglement scheme can achieve unity success probability and near-unity fidelity in the strong-coupling regime [see Fig. 3(b)] as $|r_h(\omega)| \approx 1$ and $|r_0(\omega)| \approx 1$. However, this is a challenge for QD-micropillar cavities although significant progress has been made.²² If the cavity side leakage κ_s is taken into account, the entanglement fidelity with respect to the entangled state described by Eq. (8) becomes

$$F = \frac{1}{\sqrt{1 + \frac{1}{4} \left[\frac{|r_0(\omega)|}{|r_h(\omega)|} - \frac{|r_h(\omega)|}{|r_0(\omega)|} \right]^2}}, \quad (11)$$

which is generally less than one (the coefficients $\alpha_{1,2}$ and $\beta_{1,2}$ are set to $1/\sqrt{2}$). However there can be a point where we can achieve unity fidelity as $|r_0(\omega)| = |r_h(\omega)|$ [see Fig. 3(b) dotted line]. The reflectance at this point is not in unity so the gate success probability is reduced (82% when $\kappa_s = 0.05\kappa$). However, note that $|r_0(\omega)| \neq |r_h(\omega)|$ does not affect the entanglement fidelity with respect to the entangled state described by Eq. (7) and it remains in unity even when $\kappa_s \neq 0$. By performing the single-qubit flip operation on photon 1 or 2, Eq. (7) can be transformed to Eq. (8).

IV. SUMMARY

In conclusion, we have proposed a deterministic scheme to generate polarization photon entanglement using a charged QD inside a microcavity based on giant circular birefringence and giant Faraday rotation. This scheme could be extended to generate multiphoton entangled states including GHZ and cluster states. With the proposed photon-spin entangling gate, we could also implement a deterministic photon-spin quantum interface³⁷ and a deterministic quantum controlled-NOT gate.³⁸ Therefore we could make all building blocks required for solid-state quantum networks including quantum memories, quantum repeaters, and various quantum logic gates. We believe this work opens an avenue in quantum information science.

ACKNOWLEDGMENTS

C.Y.H. thanks M. Atatüre, S. Bose, and S. Popescu for helpful discussions. J.G.R. acknowledges support from the Royal Society. This work is partly funded by EPSRC-GB IRC in Quantum Information Processing, QAP (Contract No. EU IST015848), and MEXT from Japan.

*chengyong.hu@bristol.ac.uk

¹M. A. Nielsen and I. L. Chuang, *Quantum Computation and Quantum Information* (Cambridge University Press, Cambridge, England, 2000).

²Quantum Information and Computation Roadmap, http://qist.lanl.gov/qcomp_map.shtml

³E. Knill, R. Laflamme, and G. Milburn, *Nature (London)* **409**, 46 (2001); P. Kok, W. J. Munro, K. Nemoto, T. C. Ralph, J. P. Dowling, and G. J. Milburn, *Rev. Mod. Phys.* **79**, 135 (2007).

⁴P. G. Kwiat, K. Mattle, H. Weinfurter, A. Zeilinger, A. V. Sergienko, and Y. H. Shih, *Phys. Rev. Lett.* **75**, 4337 (1995).

⁵J. Fulconis, O. Alibart, J. L. O'Brien, W. J. Wadsworth, and J. G. Rarity, *Phys. Rev. Lett.* **99**, 120501 (2007).

⁶A. Aspect, P. Grangier, and G. Roger, *Phys. Rev. Lett.* **49**, 91 (1982); A. Aspect, J. Dalibard, and G. Roger, *ibid.* **49**, 1804 (1982).

⁷O. Benson, C. Santori, M. Pelton, and Y. Yamamoto, *Phys. Rev. Lett.* **84**, 2513 (2000).

⁸R. M. Stevenson, R. J. Young, P. Atkinson, K. Cooper, D. A. Ritchie, and A. J. Shields, *Nature (London)* **439**, 179 (2006).

⁹Z. Y. Ou and L. Mandel, *Phys. Rev. Lett.* **61**, 50 (1988).

¹⁰D. Fattal, K. Inoue, J. Vučković, C. Santori, G. S. Solomon, and Y. Yamamoto, *Phys. Rev. Lett.* **92**, 037903 (2004); D. Fattal, E. Diamanti, K. Inoue, and Y. Yamamoto, *ibid.* **92**, 037904 (2004).

¹¹C.-Y. Lu, X.-Q. Zhou, O. Gühne, W.-B. Gao, J. Zhang, Z.-S. Yuan, A. Goebel, T. Yang, and J.-W. Pan, *Nat. Phys.* **3**, 91 (2007).

¹²C. Y. Hu, A. Young, J. L. O'Brien, W. J. Munro, and J. G. Rarity, *Phys. Rev. B* **78**, 085307 (2008).

¹³R. J. Warburton, C. S. Dürr, K. Karrai, J. P. Kotthaus, G. Medeiros-Ribeiro, and P. M. Petroff, *Phys. Rev. Lett.* **79**, 5282 (1997).

¹⁴C. Y. Hu, W. Ossau, D. R. Yakovlev, G. Landwehr, T. Wojtowicz, G. Karczewski, and J. Kossut, *Phys. Rev. B* **58**, R1766 (1998).

¹⁵R. M. Stevenson, R. J. Young, P. See, D. G. Gevaux, K. Cooper,

- P. Atkinson, I. Farrer, D. A. Ritchie, and A. J. Shields, *Phys. Rev. B* **73**, 033306 (2006).
- ¹⁶W. Langbein, P. Borri, U. Woggon, V. Stavarache, D. Reuter, and A. D. Wieck, *Phys. Rev. B* **69**, 161301(R) (2004).
- ¹⁷R. Seguin, A. Schliwa, S. Rodt, K. Pötschke, U. W. Pohl, and D. Bimberg, *Phys. Rev. Lett.* **95**, 257402 (2005).
- ¹⁸M. Atatüre, J. Dreiser, A. Badolato, A. Hoge, K. Karrai, and A. Imamoglu, *Science* **312**, 551 (2006); M. Atatüre, J. Dreiser, A. Badolato, and A. Imamoglu, *Nat. Phys.* **3**, 101 (2007).
- ¹⁹J. Berezovsky, M. H. Mikkelsen, O. Gywat, N. G. Stoltz, L. A. Coldren, and D. D. Awschalom, *Science* **314**, 1916 (2006).
- ²⁰G. Bester, S. Nair, and A. Zunger, *Phys. Rev. B* **67**, 161306(R) (2003).
- ²¹T. Calarco, A. Datta, P. Fedichev, E. Pazy, and P. Zoller, *Phys. Rev. A* **68**, 012310 (2003).
- ²²S. Reitzenstein, C. Hofmann, A. Gorbunov, M. Strauß, S. H. Kwon, C. Schneider, A. Löffler, S. Höfling, M. Kamp, and A. Forchel, *Appl. Phys. Lett.* **90**, 251109 (2007).
- ²³J. P. Reithmaier, G. Sęk, A. Löffler, C. Hofmann, S. Kuhn, S. Reitzenstein, L. V. Keldysh, V. D. Kulakovskii, T. L. Reinecke, and A. Forchel, *Nature (London)* **432**, 197 (2004).
- ²⁴T. Yoshie, A. Scherer, J. Hendrickson, G. Khitrova, H. M. Gibbs, G. Rupper, C. Ell, O. B. Shchekin, and D. G. Deppe, *Nature (London)* **432**, 200 (2004).
- ²⁵E. Peter, P. Senellart, D. Martrou, A. Lemaître, J. Hours, J. M. Gérard, and J. Bloch, *Phys. Rev. Lett.* **95**, 067401 (2005).
- ²⁶Z. L. Yuan, B. E. Kardynal, R. M. Stevenson, A. J. Shields, C. J. Lobo, K. Cooper, N. S. Beattie, D. A. Ritchie, and M. Pepper, *Science* **295**, 102 (2002).
- ²⁷E. Moreau, I. Robert, J. M. Gérard, I. Abram, L. Manin, and V. Thierry-Mieg, *Appl. Phys. Lett.* **79**, 2865 (2001).
- ²⁸M. Pelton, C. Santori, J. Vuckovic, B. Zhang, G. S. Solomon, J. Plant, and Y. Yamamoto, *Phys. Rev. Lett.* **89**, 233602 (2002).
- ²⁹By using a $\lambda/4$ wave plate, the photon state $|\psi^{ph}\rangle = \alpha|R\rangle + \beta|L\rangle$ can be converted to $|\psi^{ph}\rangle = \alpha|H\rangle + \beta|V\rangle$ and vice versa.
- ³⁰Photon 3 could be replaced by a weak coherent light as discussed in Ref. 12.
- ³¹A. V. Lebedev, G. Blatter, C. W. J. Beenakker, and G. B. Lesovik, *Phys. Rev. B* **69**, 235312 (2004); C. Emary, B. Trauzettel, and C. W. J. Beenakker, *Phys. Rev. Lett.* **95**, 127401 (2005).
- ³²J. R. Petta, A. C. Johnson, J. M. Taylor, E. A. Laird, A. Yacoby, M. D. Lukin, C. M. Marcus, M. P. Hanson, and A. C. Gossard, *Science* **309**, 2180 (2005); A. Greilich, D. R. Yakovlev, A. Shabaev, A. L. Efros, I. A. Yugova, R. Oulton, V. Stavarache, D. Reuter, A. Wieck, and M. Bayer, *ibid.* **313**, 341 (2006).
- ³³J. M. Elzerman, R. Hanson, L. H. Willems van Beveren, B. Witkamp, L. M. K. Vandersypen, and L. P. Kouwenhoven, *Nature (London)* **430**, 431 (2004); M. Kroutvar, Y. Ducommun, D. Heiss, M. Bichler, D. Schuh, G. Abstreiter, and J. J. Finley, *ibid.* **432**, 81 (2004).
- ³⁴C. Emary, Xiaodong Xu, D. G. Steel, S. Saikin, and L. J. Sham, *Phys. Rev. Lett.* **98**, 047401 (2007); Xiaodong Xu, Yanwen Wu, Bo Sun, Qiong Huang, Jun Cheng, D. G. Steel, A. S. Bracker, D. Gammon, C. Emary, and L. J. Sham, *ibid.* **99**, 097401 (2007).
- ³⁵J. A. Gupta, R. Knobel, N. Samarth, and D. D. Awschalom, *Science* **292**, 2458 (2001); P. C. Chen, C. Piermarocchi, L. J. Sham, D. Gammon, and D. G. Steel, *Phys. Rev. B* **69**, 075320 (2004); J. Berezovsky, M. H. Mikkelsen, N. G. Stoltz, L. A. Coldren, and D. D. Awschalom, *Science* **320**, 349 (2008).
- ³⁶H. J. Briegel and R. Raussendorf, *Phys. Rev. Lett.* **86**, 910 (2001).
- ³⁷If we send a photon in an arbitrary superposition state (i.e., $\alpha|H\rangle + \beta|V\rangle$) to interact with the spin in a known superposition state, the state of the photon is transferred to the spin by measuring the reflected photon state; similarly if we send a photon in H or V state to interact with the spin in an arbitrary superposition state, the state of the spin is transferred to the photon by measuring the spin state; C. Y. Hu, W. J. Munro, and J. G. Rarity, arXiv:0711.1431 (unpublished).
- ³⁸C. Y. Hu *et al.* (unpublished). The deterministic optical quantum controlled-NOT gate can be achieved by sending three photons: the target, the control, and the ancilla to interact with the spin, followed by measuring the spin and the ancilla photon.